Band Gap Opening of Bilayer Graphene by F4-TCNQ Molecular Doping and Externally Applied Electric Field

ARTICLE *in* THE JOURNAL OF PHYSICAL CHEMISTRY B · SEPTEMBER 2010

Impact Factor: 3.3 · DOI: 10.1021/jp102800v · Source: PubMed

3 AUTHORS, INCLUDING:

Xiaoqing Tian
Shenzhen University
10 PUBLICATIONS **98** CITATIONS

SEE PROFILE

Band Gap Opening of Bilayer Graphene by F4-TCNQ Molecular Doping and Externally Applied Electric Field

Xiaoqing Tian, Jianbin Xu,* and Xiaomu Wang

Department of Electronic Engineering and Materials Science and Technology Research Center, The Chinese University of Hong Kong, Shatin, N.T., Hong Kong SAR, P. R. China

Received: March 29, 2010; Revised Manuscript Received: June 23, 2010

The band gap opening of bilayer graphene with one side surface adsorption of F4-TCNQ is reported. F4-TCNQ doped bilayer graphene shows p-type semiconductor characteristics. With a F4-TCNQ concentration of 1.3×10^{-10} mol/cm^2, the charge transfer between each F4-TCNQ molecule and graphene is 0.45*e*, and the built-in electric field, E_{bi}, between the graphene layers could reach 0.070 V/Å. The charge transfer and band gap opening of the F4-TCNQ-doped graphene can be further modulated by an externally applied electric field (E_{ext}). At 0.077 V/Å, the gap opening at the Dirac point (*K*), $\Delta E_K = 306$ meV, and the band gap, $E_g = 253$ meV, are around 71% and 49% larger than those of the pristine bilayer under the same E_{ext}.

I. Introduction

Graphene sheet has attracted intense research interest since it was first experimentally discovered by K. S. Novoselov et al. in 2004.[1] Graphene-based nanoelectronics have been considered as a potential substitute of the conventional semiconductor-based microelectronics, due to their excellent properties, including the extremely high mobility up to 20000 cm ^{2}/V-s, close to the Dirac point and the ballistic charge transport.[1−8] However, the zero-gap characteristic has limited its applications in the electrical, optical, and magnetic areas. Therefore, how to manipulate the electronic structure of graphene is of fundamental importance. Actually, it has been reported that a band gap can be opened asymmetrically in bilayer graphene, which could be generated by a Coulomb potential difference between the two graphene layers exerted by a perpendicular electric field (E_{ext}),[9−14] although the present bottleneck of using E_{ext} to create the band gap in bilayer graphene is that the band gap is extremely small, with no more than 180 meV, as a result of E_{ext} strength confined by the limit of 0.1 V/Å for SiO_2 gate dielectric.[9]

In addition to the variable of E_{ext}, charge transfer doping is another variable affecting the band gap opening in bilayer graphene. Two effective doping approaches have been commonly applied to control the band gap opening of graphene. One method is doping with metallic species. The n-type doping effect has been successfully achieved by doping potassium in ultrathin epitaxial graphene (EG). Furthermore, the gap between its valence and conduction bands could be tuned by controlling the concentration of potassium.[15] The p-type doping effect has also been demonstrated by depositing gold atoms into graphene,[16] where the Dirac point was shifted into the unoccupied states. Unfortunately, some disadvantages induced by this method are structural conformation, defects, and clustering of dopants. Another approach for controlling the band gap opening is hydrogenation of graphene, while the deficiency of strong structural conformation has been introduced.[17−19]

How to avoid these problems caused by metal species and hydrogenation of graphene? Organic molecular surface functionalization has been found to be an effective method. For example, as recently studied by first-principles theoretical calculations and experiments, it has been found that tetracyanoethylene and tetracyanoquinodimethane (TCNQ) functionalization on graphene could achieve the band gap opening and charge transfer induced p-type doping effect.[20−22] $NH_3(CH)_6CO_2$ and $NH_3(CH)_{10}CO_2$ modification on graphene could induce a band gap into a graphene nanoribbon.[23] Previously, tetrafluorotetracyanoquinodimethane (F4-TCNQ) was proved to be an excellent candidate for functionalizing graphene to achieve the p-type doping effect, as studied by Wee et al. in performing angle-resolved photoemission spectroscopy experiments.[24] One notable advantage of employing F4-TCNQ as a strong molecular acceptor to modify the graphene surface is that no defect or strong structural conformation was created, and hence, the graphene could retain its perfect two-dimensional honeycomb structure. The other advantage is that no clustering of molecular dopants appears, due to the repulsion of charged F4-TCNQ anions between each other at high coverage. Accordingly, effective and controllable doping that maintains the extraordinarily high mobility of graphene would be accomplished by F4-TCNQ as a dopant. A F4-TCNQ-doped carbon nanotube field-effect transistor has been fabricated experimentally, and it was found that the device performances such as transconductance, on-resistance, and on/off ratio were improved by the F4-TCNQ doping effects.[25] F4-TCNQ *p*-type doping of single layer graphene has also been investigated by the first-principles method.[26]

Efforts have been previously reported to manipulate the electronic structure of bilayer graphene by E_{ext} and charge transfer-related doping separately.[9−16,20] In the present report, by applying the first principles method, we will for the first time theoretically investigate the modulation of the bilayer graphene electronic structure by combining the F4-TCNQ molecular doping and E_{ext}. To have a better understanding, the F4-TCNQ functionalized properties on bilayer graphene at low and high coverage are taken into account. The attributes of the band gap opening and charge transfer are compared among graphene sheets with the F4-TCNQ doping levels at different coverages and a pristine bilayer.

* Correspondingauthor. E-mail: jbxu@ee.cuhk.edu.hk.

10.1021/jp102800v
Published on Web 08/06/2010

II. Computational Methods

The calculations are performed within the Vienna ab initio simulation package[27] based on density functional theory. The electron−ion interaction is described by PAW potentials[28] and the plane-wave basis set, with the local density approximation (LDA) exchange-correlation functional and a cutoff energy of 29.40 Ry. Graphene bilayer modeled by $4\sqrt{3} \times 7$ supercell is used as a substrate to simulate an isolated F4-TCNQ molecule adsorption and also to represent a low coverage of 5.7×10^{-11} mol/cm^2. A supercell containing 244 atoms, which is large enough to ensure the lateral distance between the molecules, is larger than 10 Å. A vacuum layer of 1.8 nm is used to eliminate the longitudinal interactions between the super cells. To simulate a high coverage of 1.3×10^{-10} mol/cm^2, a $3\sqrt{3} \times 4$ bilayer graphene plus one F4-TCNQ molecule is applied. The sampling for the Brillouin zone includes $4 \times 4 \times 1$ and $6 \times 6 \times 1$ Monkhorst−Pack k-point for low and high coverages, respectively.

Our LDA calculations of the band gap opening of the pristine bilayer graphene under E_{ext} are in reasonable agreement with the experimental observations of a tunable band gap in the bilayer graphene.[9] LDA is better than GGA in describing a weakly bound system,[29,30] but neither GGA or LDA takes into account the van der Waals interactions. To figure out the most stable adsorption site and orientation, molecular mechanics (MM) calculations are carried out here, due to its success in treating π-conjugated molecules adsorption on the surface.[31,32] The MM+ force field, improved from MM2, is used in MM calculations. Ten highly symmetry F4-TCNQ adsorption configurations are considered, according to the orientations of the benzene ring and cyano group with respect to the hexagonal rings of graphene. Configurations with the molecular planes both parallel (lying-down) and perpendicular (edge-on) to the graphene surface are taken into account, as shown in Figure 1. The adsorption energy is calculated by the following equation:

$$\Delta E = -(E - E_0 - E_{adsorbate}) \quad (1)$$

where E is the total energy of graphene with the molecular adsorbate, $E_{adsorbate}$ is the total energy of the molecular adsorbate, and E_0 is the total energy of pristine graphene.

III. Results and Discussion

A. Adsorption Configurations of F4-TCNQ on Bilayer Graphene at Low Coverage. Figure 1 shows 10 adsorption configurations for F4-TCNQ molecules on bilayer graphene at low coverage. Comparing the corresponding calculated adsorption energies listed in Table 1, it is found that the adsorption energies of four edge-on configurations are around 0.62 eV lower than those of the lying-down ones. Consequently, the molecule prefers to adopt the lying-down configuration on the graphene in which more functional atoms of the molecule interact with the carbon atoms of graphene by partial sp^3 hybridization. Among the six lying-down configurations, the most stable adsorption is rendered by configuration e, with the largest adsorption energy of 1.95 eV. The transition from the lying-down to the edge-on configurations is very difficult due to the very large energy barrier. For a comparison, the adsorption energies of four edge-on configurations are around 0.75 eV lower than those in the lying-down cases from MM calculations. Again, the most stable one among the lying-down configurations is found to be configuration e, with the adsorption energy around 0.06−0.19 eV larger than that of other lying-down ones. For configuration e, the nitrogen atom of the cyano group is on the top of the underlying carbon atom. Such an arrangement is similar to the most stable adsorption configuration of F4-TCNQ on metal surfaces, such as Cu(111), Au(111), and Ag(111), with the cyano group on top of the metal atoms.[33,34] In configuration e, the central benzene ring of F4-TCNQ adopts laterally the relative position to the top layer graphene, which is reminiscent of the Bernal stacking of the graphene layers via $\pi-\pi$ interaction in graphite. As a reference, we also calculate the similar adsorption configurations of 2,3,5,6-tetrafluorobenzene on the graphene. The adsorption energy of configuration e is 0.37 eV, which is ~0.03−0.08 eV larger than that in other configurations.

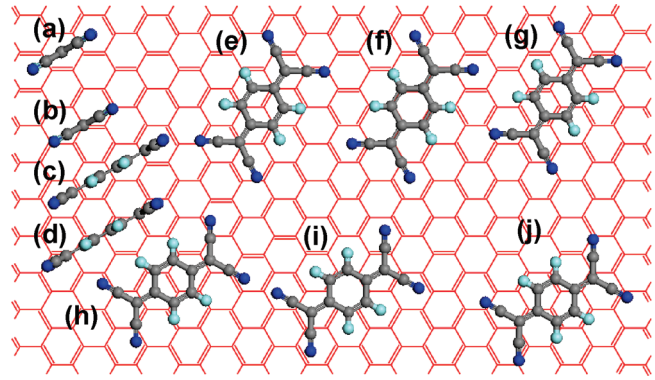

Figure 1. Top view of 10 adsorption configurations for F4-TCNQ molecules on the bilayer graphene. Nitrogen and fluorine atoms correspond to dark and light blue, carbon atoms of the F4-TCNQ molecule are gray, and carbon atoms of the top graphene layer are red.

TABLE 1: The Calculated Adsorption Energies of 10 Adsorption Configurations for F4-TCNQ on Bilayer Graphene: (1) ΔE_1(eV) for the Low Coverage; (2) ΔE_2(eV) for the High Coverage

	a	*b*	*c*	*d*	*e*	*f*	*g*	*h*	*i*	*j*
ΔE_1(eV)	1.26	1.29	1.27	1.25	1.95	1.82	1.81	1.85	1.93	1.90
ΔE_2(eV)	0.72	0.90	0.69	0.88	1.28	1.15	1.27	1.35	1.39	1.24

B. Analysis of Band Structure of F4-TCNQ-Doped Graphene at Low Coverage. To interrogate the influence of F4-TCNQ adlayer on the electronic structure of graphene, the band structure of F4-TCNQ-doped graphene with configuration e is calculated and depicted in Figure 2a. The Dirac energy level (E_D) is around 160 meV above the Fermi level, which suggests that the molecular adlayer has introduced an efficient p-type doping effect into the graphene. A direct band gap opening of $E_g = 149$ meV is found, which turns out to be $\Delta E_K = 155$ meV at the Dirac point. The illustration of the band parameters, including ΔE_K, E_g, and γ_1, are described in Figure 3a. The band structure of the bilayer graphene near the K point consists of four parabolic bands.[9−14,35] Here, E^{v1} and E^{v2} are defined as the highest and second highest occupied π orbitals. E^{c2} and E^{c2} denote the lowest and second lowest unoccupied π orbitals. E^{c1} and E^{v1} are separated by ΔE_K at the K point, whereas the minimum separation of the band gap is denoted by E_g. For a pristine bilayer graphene, both ΔE_K and E_g are equal to 0 from the band structure calculation, as depicted in Figure 2c. The other two bands, E^{c2} and E^{v2}, are separated by $2\gamma_1$. Here, γ_1 denotes the graphene interlayer tunneling energy.

As calculated, each F4-TCNQ molecule attains 0.63e from the graphene. The LUMO of F4-TCNQ is partially filled due to the charge transfer shown in the band structure. Between the top and bottom layers of the graphene, the F4-TCNQ molecule could introduce a net electric field, $E^* = E_{bi}$, where E_{bi} is the built-in electric field between the two graphene layers induced

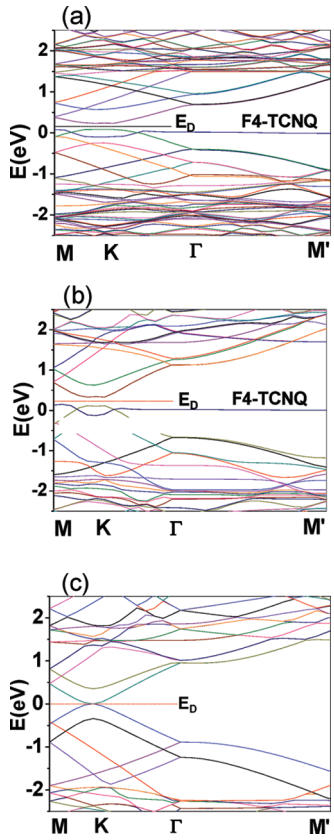

Figure 2. Band structure of the F4-TCNQ-molecule-doped bilayer graphene and pristine bilayer graphene: (a) under the low coverage, (b) under the high coverage, and (c) the pristine bilayer graphene. The Fermi level is set to zero.

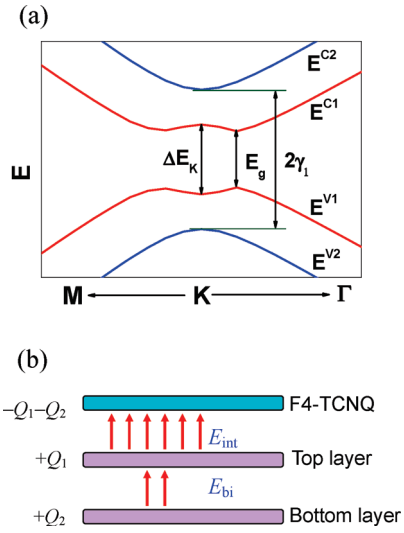

Figure 3. Band gap opening principles of F4-TCNQ molecule-doped-bilayer graphene: (a) band parameters and (b) built-in electric field distribution at zero bias.

by the bottom layer charge Q_2. The net electric field E^* breaks the potential equivalence, as shown in Figure 3b, since F4-TCNQ obtains the total charge of $Q_1 + Q_2$ from the top (Q_1) and bottom (Q_2) layer graphene. E_{int} is the total electric field between the F4-TCNQ and graphene top layer. Actually, E^* could be estimated by a tight binding model $E^* \approx \Delta E_K/d$,[10] where d is the distance between the two layers of graphene. The build-in electrostatic field is approximately perpendicular

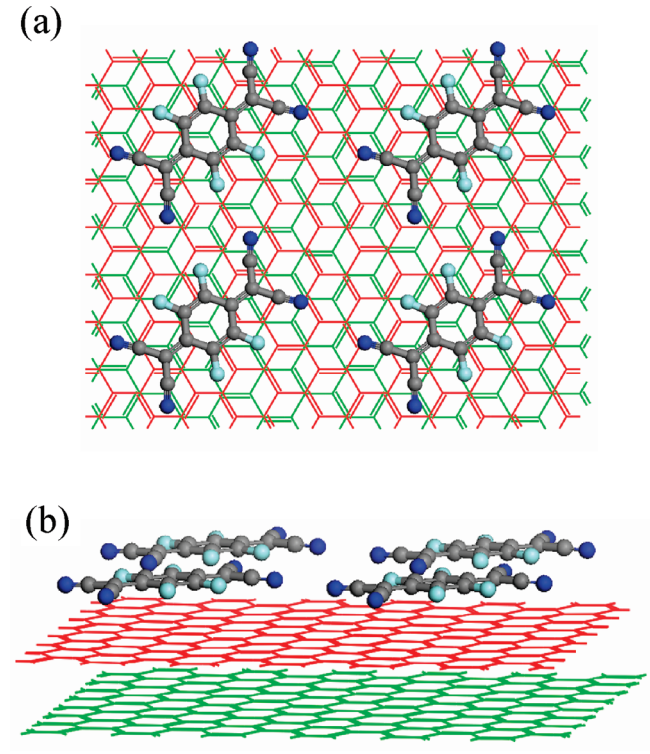

Figure 4. Optimized structure of F4-TCNQ on bilayer graphene under high coverage with 2 × 2 replicated cells: (a) top view and (b) side view. Nitrogen atoms are dark blue, fluorine atoms are light blue, carbon atoms of the F4-TCNQ molecule are gray, carbon atoms of the top graphene layer are red, and carbon atoms of the bottom graphene layer are green.

to the graphene surface, as shown in Figure 3b, solely due to the charge redistribution induced by F4-TCNQ adsorption. This interfacial electric field yields the asymmetry between the two graphene layers and results in a significant band gap opening .

C. Adsorption Configurations of F4-TCNQ on Bilayer Graphene at High Coverage. In addition to the F4-TCNQ adlayer at low coverage, the high coverage of F4-TCNQ adsorption on the graphene bilayer is investigated to provide a further comparison. The adsorption energies for 10 configurations, together with those at low coverage, are presented in Table 1. When increasing the coverage, the larger intermolecular repulsion force results in the increased total energy of molecule−substrate system, which is ascribed to the calculated average adsorption energies reduction of ∼0.6 eV. In contrast, the competition between the molecule−substrate interaction and intermolecular interaction brings about the transition of the most thermodynamically stable configuration from configuration e (Figure 3) to configuration i (Figure 4). Different from the low coverage adsorption, the most stable site is found to be site i, for high coverage adsorption, according to its adsorption energy around 0.08−0.26 eV larger than other lying-down ones obtained from MM calculation. As far as the optimized configuration (i) is concerned, the molecule is slightly rotated with respect to the graphene hexagonal ring due to the intermolecular repulsion force. The intermolecular separation is 3.2 Å. Likewise, the adsorption energy of the edge-on configuration is around 0.48 eV smaller than those lying down. Although these energies are ∼0.14 eV smaller than that in the low coverage, they are large enough to prevent the transition from the lying-down to edge-on configurations. The adsorption energies of four edge-on configurations are around 0.58 eV

lower than those in lying-down configurations, according to the results of MM calculation.

D. Comparison of Band Gap Opening between Low and High Coverages. Under high coverage, each molecule could gain 0.45*e* from the graphene. The E_D is enlarged to around 223 meV above the Fermi level, which suggests that the p-type doping effect has been enhanced, as compared with $E_D = 160$ meV at the low coverage. As depicted in Figure 2b, it is found that a band gap opening (E_g) and the gap at the Dirac point *K* (ΔE_K) are 213 and 236 meV, respectively. E^* and E_{bi} between the two graphene layers are equal, around 0.070 V/Å. In comparison with the low coverage, as shown in Figure 2a, the band gap opening is markedly enhanced.

E. Influence of F4-TCNQ Doping on Graphene Mobility. From the band structure, we could estimate the effective mass m^* of graphene electrons.[36] The m^* is proportional to the second derivative of the energy band dispersion. Near the *K* point, the m^* of the F4-TCNQ-doped bilayer is around 1.27 times that of the pristine bialyer. On the basis of the Drude model that the mobility μ is inversely proportional to m^*, so μ has been reduced around 21% by F4-TCNQ doping. Considering the mobility varies up to one order in graphene,[3] we could find that the mobility deformation induced by F4-TCNQ is moderate.

F. Electric Fields Effects on Band Gap Opening of F4-TCNQ-Doped Graphene Bilayer. To further manipulate the interfacial electronic structure between F4-TCNQ and graphene, the electric displacement field (**D**) in the range of −0.3 to 0.3 V/Å is applied perpendicularly to the graphene basal plane, corresponding to an E_{ext} of −0.077 to 0.077 V/Å, if a SiO_2 relative dielectric constant of $\varepsilon_r = 3.9$ is used as the standard relation, $\mathbf{D} = \varepsilon_r\varepsilon_0 E_{ext}$, where ε_0 is vacuum permittivity. The breakdown E_{ext} limit of SiO_2 is 0.1 V/Å, and a **D** strength of 0.27 V/Å was achieved in recent experiment.[9]

Since the electric field could alter the charge transfer between the F4-TCNQ and graphene, the hole-doping level will be enhanced or decreased, corresponding to the shifting up or down of the Dirac point relative to the Fermi level. Furthermore, the net electric field between the top and bottom layers of graphene could be tuned by an externally applied electric field, which means that the inequivalence of the top and bottom layers will be manifested. Under this condition, the net electric filed between the top and bottom layers is $E^* = (E_{bi} + \varepsilon_r E_{ext} - E_{scr})$, where E_{ext} is the externally applied electric field and E_{scr} is the screening electric field in the bilayer graphene (opposite to E_{ext}) by the induced charge. A negative E_{ext} will facilitate the electron transfer from the graphene to the F4-TCNQ, whereas a positive E_{ext} will induce the opposite process.

From Figure 5, we could find that the HOMOs under negative E_{ext} and zero bias localize mainly around the F4-TCNQ, and the HOMO under positive E_{ext} distributes on both the F4-TCNQ and graphene due to the F4-TCNQ's releasing charge to the graphene. The charge transfer between the graphene and F4-TCNQ is in the range of 0.62−0.26*e*, in response to −0.077 to 0.077 V/Å E_{ext} variation. γ_1 is in the range of 414−426 meV, following −0.077 to 0.077 V/Å E_{ext}. By comparison, the calculated γ_1 of a pristine bilayer is 350 meV, which is in good agreement with experiments.[37,38] In the pristine bilayer, the net electric field between the top and bottom layers is $E^* = (\varepsilon_r E_{ext} - E_{scr})$. The band gap opening versus E_{ext} of the pristine bilayer is depicted in Figure 6a, slightly smaller than the experimental values,[9] but in reasonable agreement. The relationship between the band gap opening versus E_{ext} for the F4-TCNQ doped bilayer under the high coverage is shown in Figure 6b. A positive electric field obviously increases the band gap opening of the graphene, whereas a negative electric field reduces it because the positive electric field constructively entrenches the E^*, and the negative electric field destructively rescinds it. As ΔE_K is increased, the calculated band gap also asymptotically follows[11]

$$E_g \approx \Delta E_K \gamma_1 / \sqrt{\Delta E_K^{\,2} + \gamma_1^{\,2}} \qquad (2)$$

For a pristine bilayer, $\Delta E_K = 179$ meV and $E_g = 170$ meV at 0.077 V/ Å, with an E^* of around 0.054 V/Å. By comparison, in the case of the doped bilayer with the high concentration of

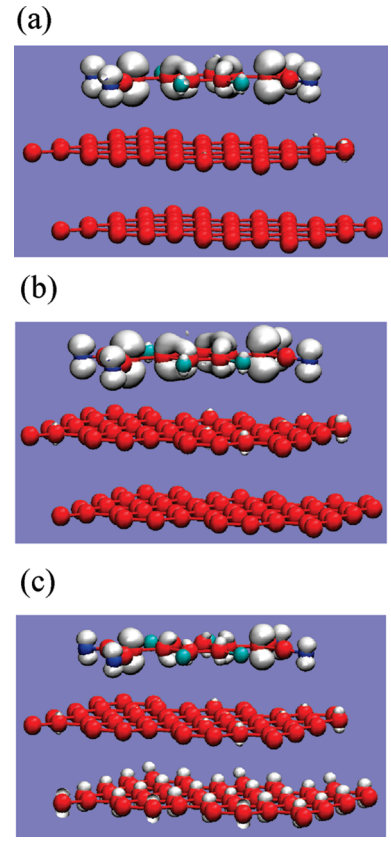

Figure 5. Cases of 0.02 e/Å^3 isosurface of charge redistribution induced by E_{ext}: (a) HOMO of −0.3 V/Å case; (b) HOMO of zero bias case; (c) HOMO of 0.3 V/Å case.

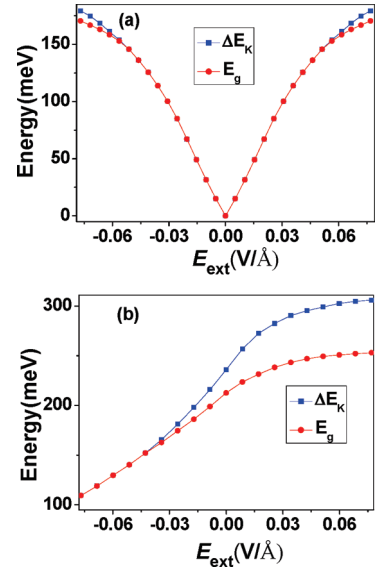

Figure 6. Effects of E_{ext} on band gap opening of bilayer graphene: (a) pristine bilayer and (b) F4-TCNQ molecule doped bilayer.

F4-TCNQ, $\Delta E_K = 236$ meV and $E_g = 213$ meV at zero bias, with an E^* of 0.070 V/Å. At 0.077 V/Å, the gap openings of the F4-TCNQ-doped bilayer are enlarged to be $\Delta E_K = 306$ meV and $E_g = 253$ meV, with $E^* = 0.095$ V/Å.

IV. Summary

In summary, we have used the first-principles technique to investigate the interfacial electronic structure between an F4-TCNQ adlayer and bilayer graphene. p-Type doped graphene is obtained by F4-TCNQ molecular doping in a bilayer graphene. The built-in electric field, E^*, between the two graphene layers by high F4-TCNQ doping could reach 0.070 V/Å, along with the gap openings $\Delta E_K = 236$ meV and $E_g = 213$ meV. By comparison, with an E_{ext} of 0.077 V/Å, the gap openings of the doped graphene are $\Delta E_K = 306$ meV and $E_g = 253$ meV, around 71% and 49% higher than their respective values for the pristine graphene bilayer under the same E_{ext}.

Acknowledgment. We gratefully acknowledge the technical assistance at the High Performance Computing Facilities of Information Technology Service Center at the Chinese University of Hong Kong, particularly Frank Ng and Stephen Chan. The work is supported in part by the Research Grants Council of Hong Kong, particularly via Grants nos. CUHK2/CRF/08, CUHK4179/10E, and CUHK4182/09E. J. B. Xu thanks the National Science Foundation of China (Grants nos. 60990314 and 60928009) for support.

Supporting Information Available: Band gap opening versus electric field for all lying-down configurations. This material is available free of charge via the Internet at http://pubs.acs.org.

References and Notes

(1) Novoselov, K. S.; Geim, A. K.; Morozov, S. V.; Jiang, D.; Zhang, Y.; Dubonos, S. V.; Grigorieva, I. V.; Firsov, A. A. *Science* **2004**, *306*, 666.

(2) Castro Neto, A. H.; Guinea, F.; Peres, N. M. R.; Novoselov, K. S.; Geim, A. K. *Rev. Mod. Phys.* **2009**, *81*, 109.

(3) Geim, A. K.; Novoselov, K. S. *Nat. Mater.* **2007**, *6*, 183.

(4) Pan, Y.; Zhang, H. G.; Shi, D. X.; Sun, J. T.; Du, S. X.; Liu, Fe.; Gao, H. J. *Adv. Mater.* **2009**, *21*, 2777.

(5) Yang, L.; Deslippe, J.; Park, C.-H.; Cohen, M. L.; Louie, S. G. *Phys. Rev. Lett.* **2009**, *103*, 186802.

(6) Kudin, K. N.; Ozbas, B; Schniepp, H. C.; Prud'homme, R. K.; Aksay, I. A.; Car, R. *Nano Lett.* **2008**, *8*, 36.

(7) Yan, J; Zhang, Y.; Kim, P.; Pinczuk, A. *Phys. Rev. Lett.* **2007**, *98*, 166802.

(8) Yan, Q. M.; Huang, B.; Yu, J.; Zheng, F. W.; Zang, J.; Wu, J.; Gu, B. L.; Liu, F.; Duan, W. H. *Nano Lett.* **2007**, *6*, 1469.

(9) Mak, K. F.; Lui, C. H.; Shan, J.; Heinz, T. F. *Phys. Rev. Lett.* **2009**, *102*, 56405.

(10) Gava., P.; Lazzeri, M.; Saitta, A. M.; Mauri, F. *Phys. Rev. B* **2009**, *79*, 165431.

(11) Min, H; Sahu, B.; Banerjee, S. K.; MacDonald, A. H. *Phys. Rev. B* **2007**, *75*, 155115.

(12) McCann, E. *Phys. Rev. B* **2006**, *74*, 161403(R).

(13) Castro, E. V.; Novoselov, K. S.; Morozov, S. V.; Peres, N. M. R.; Lopes dos Santos, J. M. B.; Nilsson, J.; Guinea, F.; Geim, A. K.; Castro Neto, A. H. *Phys. Rev. Lett.* **2007**, *99*, 216802.

(14) Avetisyan, A. A.; Partoens, B.; Peeters, F. M. *Phys. Rev. B* **2009**, *79*, 035421.

(15) Ohta, T.; Bostwick, A.; Seyller, T.; Horn, K.; Rotenberg, E. *Science* **2006**, *313*, 951.

(16) Gierz, I.; Riedl, C.; Starke, U.; Ast, C. R.; Kern, K. *Nano Lett.* **2008**, *8*, 4603.

(17) Elias, D. C.; Nair, R. R.; Mohiuddin, T. M. G.; Morozov, S. V.; Blake, P.; Halsall, M. P.; Ferrari, A. C.; Boukhvalov, D. W.; Geim, A. K.; Novoselov, K. S. *Science* **2009**, *323*, 610.

(18) Zhou, J.; Wu, M. M.; Zhou, X.; Sun, Q. *Appl. Phys. Lett.* **2009**, *95*, 103108.

(19) Sofo, J. O.; Chaudhari, A. S.; Barber, G. D. *Phys. Rev. B* **2007**, *75*, 153401.

(20) Lu, Y. H.; Chen, W.; Feng, Y. P.; He, P. M. *J. Phys. Chem. B* **2009**, *113*, 2.

(21) Manna, A. K.; Pati, S. K. *Chem.—Asian J.* **2009**, *4*, 855.

(22) Varghese, N.; Ghosh, A.; Voggu, R.; Ghosh, S.; Rao, C. N. R. *J. Phys. Chem. C* **2009**, *113*, 16855.

(23) Dalosto, S. D.; Levine, Z. H. *J. Phys. Chem. C* **2008**, *112*, 8196.

(24) Chen, W.; Chen, S.; Qi, D. C.; Gao, X. Y.; Wee, A. T. S. *J. Am. Chem. Soc.* **2007**, *129*, 10418.

(25) Nosho, Y.; Ohno, Y.; Kishimoto, S.; Mizutani, T. *Nanotechnology* **2007**, *18*, 415202.

(26) Pinto, H.; Jones, R.; Goss, J. P.; Briddon, P. R. *J. Phys.: Condens. Matter* **2009**, *21*, 402001.

(27) Kresse, G. *Furthmü ller J. Comput. Mater. Sci.* **1996**, *6*, 15.

(28) Kresse, G.; Joubert, D. *Phys. Rev. B* **1999**, *59*, 1758.

(29) Rochefort, A.; Wuest, J. D. *Langmuir* **2009**, *25*, 210.

(30) Li, M. M.; Zhang, J.; Li, F. J.; Zhu, F. X.; Zhang, M.; Zhao, X. F. *Phys. Status Solidi C* **2009**, *6*, s90.

(31) Shi, D. X.; Ji, W.; Lin, X.; He, X. B.; Lian, J. C.; Gao, L.; Cai, J. M.; Lin, H.; Du, S. X.; Lin, F.; Seidel, C.; Chi, L. F.; Hofer, W. A.; Fuchs, H.; Gao, H.-J. *Phys. Rev. Lett.* **2006**, *96*, 226101.

(32) Ulbricht, H.; Moos, G.; Hertel, T. *Phys. Rev. Lett.* **2003**, *90*, 095501.

(33) Romaner, L.; Heimel, G.; Bre'das, J. L.; Gerlach, A.; Schreiber, F.; Johnson, R. L.; Zegenhagen, J.; Duhm, S.; Koch, N.; Zojer, E. *Phys. Rev. Lett.* **2007**, *99*, 56801.

(34) Rangger, G. M.; Hofmann, O. T.; Romaner, L.; Heimel, G.; Bröker, B.; Blum, R. P.; Johnson, R. L.; Koch, N.; Zojer, E. *Phys. Rev. B* **2009**, *79*, 165306.

(35) Malard, L. M.; Nilsson, J.; Elias, D. C.; Brant, J. C.; Plentz, F.; Alves, E. S.; Castro Neto, A. H.; Pimenta, M. A. *Phys. Rev. B* **2007**, *76*, 201401.

(36) Wallace, P. R. *Phys. Rev.* **1947**, *71*, 622.

(37) Kuzmenko, A. B.; Van Heumen, E.; Van der Marel, D.; Lerch, P.; Blake, P.; Novoselov, K. S.; Geim, A. K. *Phys. Rev. B* **2009**, *79*, 115441.

(38) Malard, L. M.; Nilsson, J.; Elias, D. C.; Brant, J. C.; Plentz, F.; Alves, E. S.; Castro Neto, A. H.; Pimenta, M. A. *Phys. Rev. B* **2007**, *76*, 201401.

JP102800V